THE JOURNAL OF PHYSICAL CHEMISTRY B

Article

pubs.acs.org/JPCB

On the Mechanisms of Triplet Excited State Population in 8-Azaadenine

João Paulo Gobbo* and Antonio Carlos Borin

Instituto de Química, Universidade de São Paulo, and NAP-PhotTech, the USP Consortium for Photochemical Technology, Av. Prof. Lineu Prestes 748, 05508-900 São Paulo, São Paulo, Brazil

Supporting Information

ABSTRACT: The photophysics of 8-azaadenine (8-AA) has been studied with the CASPT2//CASSCF protocol and ANO-L double-ζ basis sets. Stationary equilibrium structures, surface crossings, minimum energy paths, and linear interpolations have been used to study possible mechanisms to populate the lowest triplet state, T_1 $^3(\pi\pi^*)$, capable of sensitizing molecular oxygen. Our results show that two main mechanisms can occur after photoexcitation to the S_2 $^1(\pi\pi^*)$ state. The first one is through the S_2/S_1 conical intersection $(({}^1\pi\pi^*/{}^1n\pi^*)_{CI})$, leading to the S_1 $({}^1n\pi^*)$ state minimum, $(S_1\ ({}^1n\pi^*))_{min}$, where a singlet−triplet crossing, $({}^1n\pi^*/{}^3\pi\pi^*)_{STC}$, is accessible. The second one starts with the $({}^1\pi\pi^*/{}^3n\pi^*)_{STC}$ at the $(S_2({}^1\pi\pi^*))_{min}$, from which the system can evolve to the $(T_2\ ({}^3n\pi^*))_{min}$, with subsequent population of the T_1 excited electronic state, due to the $({}^3n\pi^*/{}^3\pi\pi^*)_{CI}$ conical intersection.

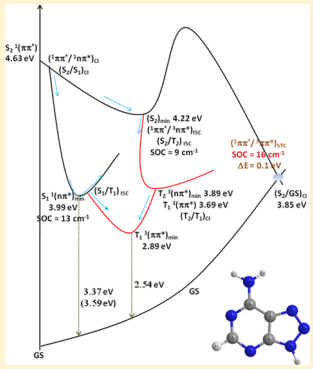

1. INTRODUCTION

The interaction of light with DNA or RNA has been studied by many scientists[1] due to its implications for human health and fundamental science such as natural selection, for instance. Nowadays, it is known that DNA and RNA photostability is intrinsically related to the structure of their nucleic acid bases constituents. In the early seventies, Daniels and Hauswirth[2] pointed out that canonical nucleobases (NABs) have very low fluorescence quantum yields, a fact confirmed and reviewed later by other authors.[3,4] More recently, modern spectroscopic techniques[1] have suggested that the photophysics of the NABs is ruled by a common ultrafast decay pattern. Theoretically, these systems have been studied by several research groups.[5−11] Serrano-Andrés et al.[5−8] proposed, on the basis of accurate multiconfigurational calculations, that after population of the bright singlet excited state, $^1(\pi\pi^*)$, by UV radiation geometrical distortions lead the system, in a barrierless manner, to a region where a crossing with the ground state hypersurface takes place. Acting as funnels, these crossings or conical intersections (CIs)[12,13] may transfer the energy from the $^1(\pi\pi^*)$ excited state back to the closed shell ground state hypersurface, with subsequent vibrational relaxation to its equilibrium structure.

Modifications of the covalent skeleton or the structural arrangement of the NABs may result in compounds with very different optical properties.[14−17] A typical well established example is the difference in fluorescent properties of adenine and its constitutional isomer, 2-aminopurine (2AP).[1] Although adenine has a very low quantum yield of fluorescence ($\Phi_F \approx 3 \times 10^{-4}$),[1,4,18−22] 2AP presents a $\Phi_F = 0.66$ in water.[23,24] Serrano-Andrés et al. showed that the existence of a local minimum in the $^1(\pi\pi^*)$ excited surface of 2AP was responsible for its fluorescence properties,[5] whereas in adenine such a minimum is not present.

The so-called aza-nucleobases are obtained by substituting a carbon atom of the molecular skeleton by a nitrogen atom. Their importance comes from their potential use to treat several diseases,[25,26] including different types of cancer.[27,28]

Recently, Suzuki and co-workers[17,29] reported a study characterizing the excited states of four aza-nucleobases [6-azauracil (6-AU), 8-azaadenine (8-AA: Figure 1), 5-azacytosine (5-AC), and 8-azaguanine (8-AG)] in acetronitrile on the basis of absorption and emission spectra, laser flash photolysis, and time-dependent density functional theory (TD-DFT). In relation to 8-AA, the authors concluded that, when the $^1(\pi\pi^*)$ state is populated by 248 nm laser irradiation, the system evolves to a triplet state $^3(8AA^*)$ with a substantial quantum yield of intersystem crossing (Φ_{ISC}) and produces singlet oxygen with moderate efficiency ($\Phi_\Delta = 0.15 \pm 0.02$). The emissive properties of 8-AA was also discussed by the authors, who reported an emission band maximum near 350 nm (3.55 eV) with a fluorescence quantum yield (Φ_F) of $3.2 \pm 0.4 \times 10^{-3}$. The TD-DFT calculations found several singlet and triplet states in the energy region up to 5.15 eV, confirming the existence of a dark $^1(n\pi^*)$ state assumed to play an important role in the photophysics of 8-AA and 6-AU.

Our group has focused on describing the photophysical properties of aza-nucleobases in the last years. In particular, we described the mechanism of triplet excited state population of 6-AU.[30] In short, after initial population of the bright $^1(\pi\pi^*)$

Received: September 14, 2012
Revised: November 8, 2012
Published: November 13, 2012

dx.doi.org/10.1021/jp3091599 | J. Phys. Chem. B 2012, 116, 14000−14007

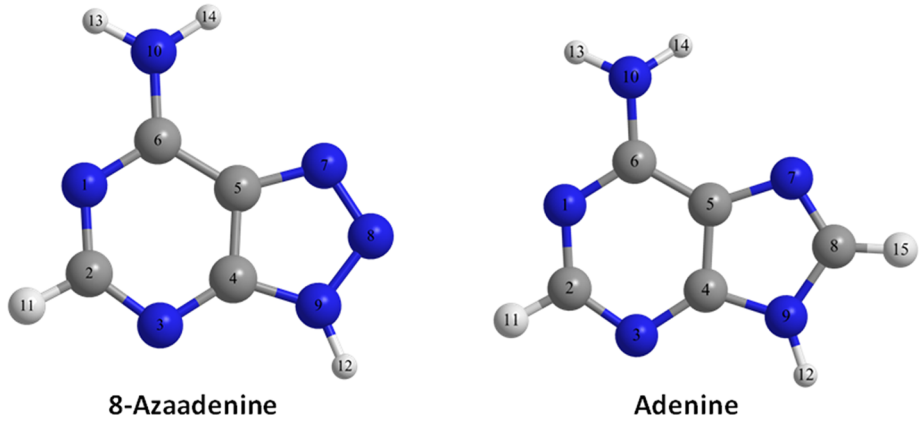

Figure 1. Schematic structure and labeling of 8-azaadenine (8-AA) and adenine.

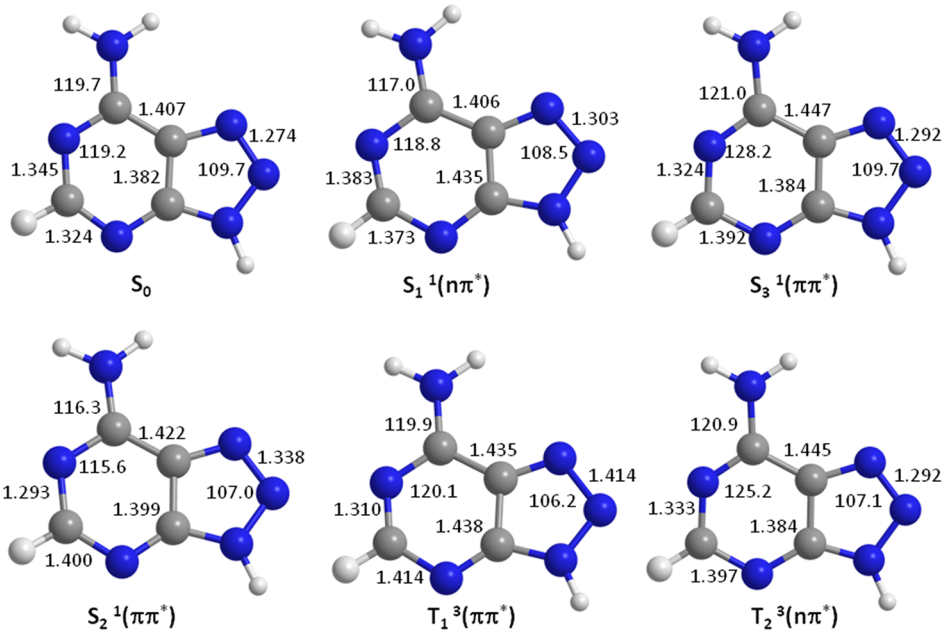

Figure 2. Optimized bond distances (Å) and angles (degrees) of lower singlet and triplet electronic states of 8-AA.

state, the system evolves to a region of the $^1(\pi\pi^*)$ hypersurface where two crossings are readily accessible: $(^1n\pi^*/^1\pi\pi^*)_{CI}$ and $(^3n\pi^*/^1\pi\pi^*)_{STC}$. Via these crossings, the 8-AA* can relax to the respective state minima, $^1(n\pi^*)_{min}$ or $^3(n\pi^*)_{min}$, where new crossings, $(^3\pi\pi^*/^1n\pi^*)_{STC}$ or $(^3\pi\pi^*/^3n\pi^*)_{CI}$, are also accessible, leading to T_1 $^3(\pi\pi^*)$ state, responsible for the observed photosensitization of oxygen.[17]

In this contribution, we describe our results for the photophysical mechanisms of population of the triplet manifold of 8-AA, based on the computation of important stationary structures (state energy minimum, conical intersections, and singlet−triplet crossings) and the connectivity between them through minimum energy paths (MEPs) or linear interpolation in internal coordinate calculations as well as the magnitude of spin−orbit coupling (SOC)[31] in some selected geometries. As done previously for 6-AU,[30] the calculations were carried out with the CASPT2//CASSCF protocol. Whenever appropriate, a comparison with adenine was also made.

2. METHODOLOGY

The most relevant optimized structures, conical intersections (CI), minimum energy paths (MEPs), and intersystem crossings (ISCs) were obtained at the Complete Active Space Self Consistent Field (CASSCF) level of theory.[32] Dynamical correlation effects were incorporated into the computed vertical transition energies with the Second-Order Multiconfigurational Perturbation Theory Approach (CASPT2).[33,34] This strategy, the so-called CASPT2//CASSCF protocol, has been successfully applied in several other applications.[30,35−37]

The inclusion of all electrons and orbitals of π (12 electrons and 10 orbitals) and n (8 electrons and 4 orbitals) characters would result in an active space comprising 20 electrons and 14 orbitals (CAS(20,14)), which is not feasible. Therefore, it was necessary to carry out a systematic study to choose the smallest active space that encompasses the most relevant orbitals only. After considering different active spaces, aiming to investigate the stability of the energies in relation to the size of the active space, we decided to employ an active space with the full π system plus three n orbitals (CAS(18,13)) for computing the relevant vertical and adiabatic energies values. However, for geometry optimizations (minima and conical intersections), as well as for the points along the MEPs, this active space would imply very time-consuming calculations. Therefore, the geometry optimizations were computed with an active space

dx.doi.org/10.1021/jp3091599 | J. Phys. Chem. B 2012, 116, 14000−14007

Table 1. Bond Distances (Å) for the Ground and Lower Excited States of Adenine, 8-Azaadenine, and Its Tautomer 8H-8-Azaadenine

	N_1-C_2	C_2-N_3	N_3-C_4	C_4-C_5	C_5-C_6	C_6-N_{10}	C_6-N_1	C_5-N_7	N_7-N_8	N_8-N_9	N_9-C_4
8-azaadenine											
S_0	1.345	1.324	1.331	1.382	1.407	1.355	1.321	1.374	1.274	1.341	1.353
[29]	1.346	1.336	1.346	1.398	1.422	1.339	1.350	1.370	1.302	1.361	1.357
[48]	1.334	1.311	1.332	1.373	1.408	1.335		1.368	1.252	1.344	
S_1	1.383	1.373	1.322	1.435	1.406	1.352	1.377	1.347	1.303	1.358	1.356
S_2	1.293	1.400	1.343	1.399	1.422	1.331	1.421	1.340	1.338	1.343	1.334
S_3	1.324	1.392	1.337	1.384	1.447	1.369	1.320	1.340	1.292	1.360	1.336
T_1	1.310	1.414	1.280	1.438	1.435	1.357	1.342	1.300	1.414	1.349	1.367
T_2	1.333	1.397	1.332	1.384	1.445	1.371	1.309	1.342	1.292	1.357	1.377
8H-8-azaadenine											
S_0	1.378	1.300	1.359	1.403	1.434	1.357	1.298	1.329	1.312	1.313	1.331
[48]	1.362	1.288	1.356	1.397	1.431	1.337		1.322	1.289	1.308	
adenine											
[8]	1.347	1.311	1.342	1.375	1.416	1.347	1.309	1.382	1.320	1.369	1.364

further reduced to CAS(16,12), comprising only nine π orbitals plus three n orbitals, by moving the π orbital localized on the NH_2 group from the previous active space (CAS(18,13)) to the inactive space, based on energy and occupation number criteria, as it was done in previous computational studies related to adenine.[5]

Minimum energy paths on the $^1(\pi\pi)^*$ excited states surfaces were obtained at the CAS(12,10) level, considering only the π, π^* orbitals and electrons active, with a modified version of the steepest descendent algorithm developed by Anglada and Boffil, as proposed by Müller-Brown. Mass-weighted coordinates (in bohr $(amu)^{1/2}$) were used, which makes the MEPs computed in this contribution equivalent to the so-called intrinsic reaction coordinate (IRC). At the obtained points, CASPT2 calculations on several singlet and triplet states were carried out in order to incorporate dynamical correlation effects.[38−40] Whenever MEPs calculations were not possible, linear interpolations in internal coordinates were carried out to study the electronic states along the path connecting the two structures of interest. For each optimized structure, dynamical correlation effects were introduced in the wave function via single point CASPT2(18,13) calculations (18 electrons in 3 n orbitals and 10 π and π^* orbitals). An imaginary shift[41] of 0.2 au was used to avoid intruder states and no IPEA shift[42] (ionization potential−electron affinity shift) was employed, to be consistent with previous studies.

Conical intersections not obtained along the MEPs were computed at the CASSCF level imposing the restriction of degeneracy between the two states considered, employing the restricted Lagrange multipliers technique;[38] no nonadiabatic coupling elements were computed. Spin−orbit couplings (SOCs) were computed within the AMFI (atomic mean field integrals) framework.[43] Solvent effects were taken into account with the polarized continuum model (PCM) model.[44,45]

Calculations were done with the MOLCAS-7.4 software,[46] employing atomic natural orbital (ANO-L)[47] basis sets of double-ζ quality plus polarization, being described as C,N,O (10s6p3d)/H (7s3p) primitive gaussians contracted to C,N,O (3s2p1d)/H (2s1p). All computations were performed by imposing no symmetry restrictions (C_1 point group).

3. RESULTS AND DISCUSSION

Stationary Points. The optimized ground and selected excited states structures are shown in Figure 2 and the most relevant parameters collected in Table 1. The optimized geometry of the 8-AA ground state is computed to be planar. Our results are in agreement with the TD-DFT and HF results of Kobayashi et al.[29] and Contreras et al.[48] Comparing with adenine,[8] the most discrepant bond lengths are those related to the exchange of the carbon by a nitrogen atom ((N_7-C_8) = 1.320 Å and $d(C_8-N_9)$ = 1.369 Å at the CASSCF level[8]).

The 9H-8-azaadenine (hereafter called 8-azaadenine), 8H-8-azaadenine, and 7H-8-azaadenine tautomers were studied by Contreras et al.[48] at the MP2/6-31G*//HF/6-31G* level in the gas phase and aqueous solution. In the gas phase, the authors found that the most stable tautomer is 9H, followed by 8H (0.043 eV, higher in energy), with 7H-azaadenine 0.31 eV above the 9H tautomer. In aqueous solution, the stability depends on the model used to study the solvent effects. Using the Self-Consistent Reaction Field (SCRF) model, the authors found the 9H as the most stable isomer, but 8H-8-azaadenine is more stable by 0.016 eV with the Isodensity Surface Polarized Continuum (IPCM) model.[48] The authors concluded that in future work concerning the tautomers only the 9H and 8H tautomers have to be considered.

The geometrical parameters obtained by us (Table 1) for 8H-8-azaadenine are in agreement with the results reported by Contreras et al.,[48] with a maximum difference of 0.023 Å for the N_7-N_8 bond distance. As expected, comparing the two tautomers, an increase in the N_7-N_8 bond length is observed ($\Delta d(N_7-N_8)$ = 0.38 Å), which can be attributed to a change in the bond order from double to single character. In the gas phase, at the CASPT2//CASSCF level, the 9H isomer is found to be more stable than the 8H one by 0.13 eV. For completeness, the electronic spectrum of the 8H tautomer in the Franck-Condom region was also taken into account. The S_1 state is computed to be a $^1(n\pi^*)$ state, located 4.14 eV above the ground state. Close to S_1, the allowed S_2 state (f = 0.224) exhibits a $^1(\pi\pi^*)$ (HOMO − LUMO) character, being placed 4.55 eV above the ground state. Due to its large dipole moment (μ = 7.36 D), it is prone to large solvation effects.

Since our results suggest that the energy of the 9H isomer is lower than that of 8H and the experimental excitation spectrum in acetonitrile solution[29] does not exhibit evidence of the presence of any other tautomer, our attention will focus only on the photophysical properties of the 9H isomer and its cytotoxic activity due to $^1O_2$ production.

dx.doi.org/10.1021/jp3091599 | J. Phys. Chem. B 2012, 116, 14000−14007

Table 2. Singlet and Triplet States of 8-Azaadenine and Adenine: Vertical Excitation Energy (E_{VA}, eV), Vertical Excitation Energy in Acetronitrile (E_{VAS}, eV), Experimental Vertical Excitation Energy (E_{VAS}, eV), Oscillator Strengths (f), Dipole Moments (μ, D), and Relaxed Emission, from the Excited State Relaxed Geometry (R.emi, eV)

8-azaadenine absorption								adenine absorption			
	this work				ref 29				refs 5 and 6		
state	E_{VA}	E_{VAS}	f	μ	E_{VAS}[a]	E_{VAE}	f	state	E_{VA}	f	μ
S_0	0.00	0.00		0.52	0.00				0.00		2.67
$S_1(n\pi^*)$	4.51	4.65	0.001	2.30	4.53			$S_1(n\pi^*)$	4.96	0.0037	1.99
								$S_2(\pi\pi^*)$	5.16	0.0042	2.46
$S_2(\pi\pi^*)$	4.63	4.55	0.284	3.24	4.55	4.51	0.2144	$S_3(\pi\pi^*)$	5.35	0.1747	4.17
$S_3(\pi\pi^*)$	4.83	4.82	0.025	1.00	5.14	4.82	0.0228				
$S_4(n\pi^*)$	5.19	5.36		1.39	5.00						
$T_1(\pi\pi^*)$	3.73	3.66		0.61	3.16				4.00		
$T_2(n\pi^*)$	4.15			0.85	4.08				4.91		
$T_3(\pi\pi^*)$	4.59			1.03	4.41				4.95		
$T_4(n\pi^*)$	4.80			1.62							

8-azaadenine emission			
	R.emi	ref 29.	ref 49. (expt)
$S_1(n\pi^*)$	3.37	3.55	3.59
$T_1(\pi\pi^*)$	3.54		

[a] B3LYP/6-31G+(d,p)/PCM.

The lowest 8-AA singlet excited state (S_1) is a $^1(n\pi^*)$ state (Table 2), derived from the ground state by a single excitation from the nonbonding n orbital (Figure 3, n_1 and n_2 involving the N_1, N_3, and N_7 atoms) to the LUMO orbital of the π skeleton. Unlike the analysis carried out by Kobayashi et al.[29] based on DFT calculations, our results suggest that the N_8 electron pair plays a minor role in the electronic transition. In the Franck−Condon region, the S_1 state is placed 4.51 eV (Table 2) above the S_0 minimum in the gas phase. When considering 8-AA in acetonitrile, the S_1 excitation energy experiences a blue-shift of 0.14 eV, to 4.65 eV, in line with the DFT value (4.53 eV) reported in the literature.[29]

The minimum of the S_1 state potential energy surface, $(S_1)_{min}$, is located adiabatically 3.99 eV above the ground state. Based on the very low Φ_F in acetonitrile (3.2×10^{-3})[29] and water (8×10^{-3}),[49] 8-AA is, essentially, a nonfluorescent chromophore. The vertical energy difference at this geometry, $\Delta E(S_1-S_0)$, is 3.37 eV, which can be compared to the reported experimental maximum wavelength of fluorescence of 8-azaadenosine in water of 3.59 eV.[49] In comparison to the ground state (Table 1), the geometrical parameters of the $(S_1)_{min}$ show mainly an elongation of the C_4-C_5 (Δd = 0.053 Å), N_7-N_8 (Δd = 0.029 Å), and N_1-C_2 (Δd = 0.038 Å) bond distances.

In the gas phase, the allowed S_2 $^1(\pi\pi^*)$ (μ = 3.24 D) state is computed vertically at 4.63 eV above the S_0 state, while in acetonitrile it is placed at 4.55 eV (4.55 eV TD-DFT[29]), in line with the experimental value (4.51 eV),[29] corresponding to a small red-shift of 0.08 eV. In comparison to the ground state, the S_2 $^1(\pi\pi^*)$ state is obtained by a single excitation related to a HOMO − LUMO transition (Figure 3), with an associated oscillator strength of 0.284. As to the geometrical parameters, the largest variations are observed for the N_7-N_8, C_2-N_3, and C_6-N_1 bond distances, which increase by 0.064, 0.076, and 0.100 Å, respectively. For the sake of completeness, the S_3 $^1(\pi\pi^*)$ state was also considered in this work and its geometrical parameters are given in Figure 2 and Table 1.

The comparison between the S_1 $^1(n\pi^*)$ and S_2 $^1(\pi\pi^*)$ excited states of 8-AA and adenine reveals some differences

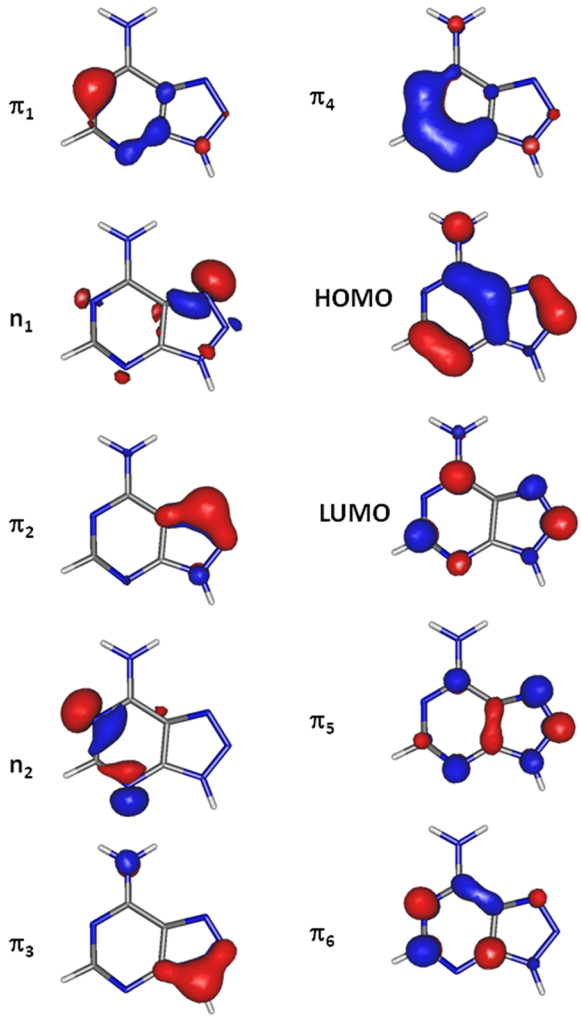

Figure 3. Most important valence molecular orbitals for 8-AA in the ground state equilibrium structure.

dx.doi.org/10.1021/jp3091599 | J. Phys. Chem. B 2012, 116, 14000−14007

worth noting (Table 2). Comparing the excitation energies of adenine and 8-AA, the excited states of adenine are located approximately 0.5 eV higher in energy. Another difference is the energetic order of the allowed $^1(\pi\pi^*)$ state which is the lowest one for 8-AA ($S_2(\pi\pi^*)$, E = 4.63 eV and f = 0.284), while in adenine it corresponds to the second one ($S_3(\pi\pi^*)$, E = 5.35 eV and f = 0.1747).[4]

For 8-AA, the T_1 $^3(\pi\pi^*)$ is derived from the ground state by a single HOMO → LUMO excitation, like the S_2 $^1(\pi\pi^*)$, but with different spin coupling. Located 3.73 eV above the ground state in the gas phase, it is higher than the DFT value[29] (3.16 eV), with about the same discrepancy (0.5 eV) between our results (CASPT2//CASSCF protocol) and those computed at DFT level[2] for the triplet excited states of 6-AU.[30]

The minimum energy structure for the T_1 $^3(\pi\pi^*)$ state exhibits an increase of the C_2-N_3 (Δd = 0.090 Å), C_4-C_5 (Δd = 0.056 Å), and N_7-N_8 (Δd = 0.140 Å), and a contraction of the N_3-C_4 (Δd = −0.051 Å) and C_5-N_7 (Δd = −0.074 Å) bond lengths (Table 1 and Figure 2) compared to S_0, and exhibits an alternation of bond order. The next triplet state, T_2 $^3(n\pi^*)$, has a large participation of the N_8 nonbonding electrons in the relevant orbitals that describe the transition, contrary to what is observed for the first singlet $^1(n\pi^*)$ state. Computed to be 4.15 eV (DFT: 4.08 eV[29]) above the ground state, its dipole moment (μ = 0.85 D) is slightly larger than that computed for the ground state. Its equilibrium structure is characterized by large C_2-N_3 (1.397 Å) and C_5-C_6 (1.445 Å) bond distances.

Although adenine presents a negligible value of Φ_Δ, due to its known photostability and very low quantum yield for triplet population,[6] its triplet states (Table 2) show the same trends observed for 8-AA. The lowest triplet excited state of adenine is a $^3(\pi\pi^*)$ state at 4.00 eV, followed by a $^3(n\pi^*)$ state at 4.91 eV. The triplet energies of adenine are placed at much higher energies than those of 8-AA, by up to 0.76 eV.

Mechanisms of Population of the Triplet States and Energy Relaxation. Kobayashi et al. suggested the existence of two types of aza-nucleobases (types A and B), depending on whether the $^1(n\pi^*)$ excited state is located below the first $^1(\pi\pi^*)$ state or not. According to this classification, Type A nucleobases (6-azauracil and 8-azaadenine) have a low lying $^1(n\pi^*)$ state below the first $^1(\pi\pi^*)$ state, whereas the type B nucleobases (5-azacytosine and 8-azaguanine) do not. The presence of a low-lying $^1(n\pi^*)$ excited state is the key point to explain the transfer of energy to the triplet manifold.[29] The 8-AA and 6-AU[17,29,30,50] species generate $^1O_2$ with Φ_Δ = 0.15 and Φ_Δ = 0.63, respectively, due to a low-lying triplet state with enough energy to excite molecular oxygen. Thus, the mechanisms of energy relaxation observed in DNA[8,36] and aza-nucleobases studied by Kobayashi et al.[17,29] are encrypted in the $^1(n\pi^*)$, $^1(\pi\pi^*)$, $^3(n\pi^*)$, and $^3(\pi\pi^*)$ excited states.

According to our results for the gas phase, 8-AA is photoexcited to the S_2 $^1(\pi\pi^*$ - HL) (f = 0.284), its allowed state, computed to be 4.63 eV above the ground state minimum. The MEP of the S_2 $^1(\pi\pi^*)$ state, starting at the Franck−Condon region, is shown in Figure 4 (red circles), together with the energy profile of the S_1 ($^1(n\pi^*)$, blue up triangles), T_1 ($^3(\pi\pi^*)$, green down triangles), and T_2 ($^3(n\pi^*)$, inclined pink triangles) excited states along the same coordinates. As can be seen, the S_2 state evolves barrierlessly toward its minimum, $(S_2)_{min}$, located adiabatically 4.22 eV above the ground state, from which radiative emission should

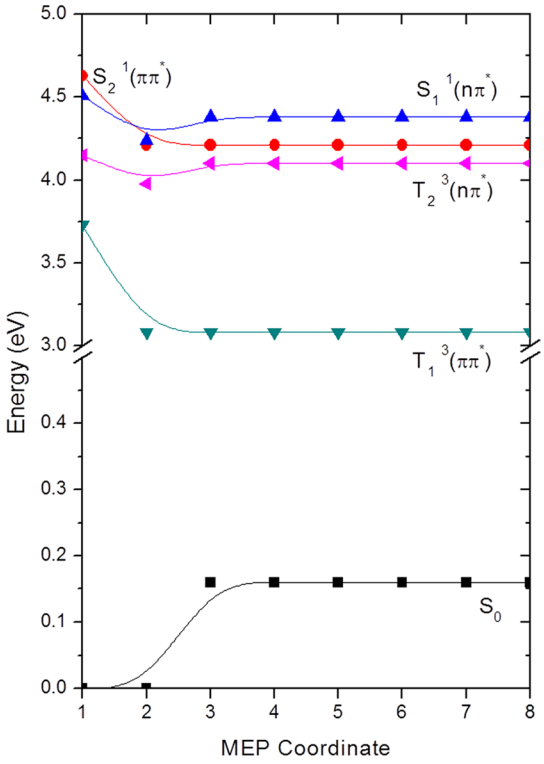

Figure 4. Evolution of ground state (black squares), S_1 ($^1(n\pi^*)$, blue triangles), T_1 ($^3(\pi\pi^*)$, upside down green triangle), and T_2 ($^3(\pi\pi^*)$, inclined pink triangles) along the minimum energy path of the S_2 ($^1(\pi\pi^*)$, red circles).

be possible. However, experimental results indicate only a very weak fluorescence ($\Phi_F \approx 10^{-3}$) centered in another energetic region (3.55[29] and 3.59 eV[49]), suggesting that another state must be responsible for the radiative decay.

As mentioned before, the evolution of the initially populated S_2 $^1(\pi\pi^*)$ state from the Franck−Condon geometry was characterized by computing the MEP along its hypersurface (Figure 4). At the very beginning of the MEP (Figure 4), the S_2 $^1(\pi\pi^*)$ state goes barrierless to a planar conical intersection (ΔE = 0.12 eV) involving the S_1 $^1(n\pi^*)$ and S_2 $^1(\pi\pi^*)$ states, $(^1n\pi^*/^1\pi\pi^*)_{CI}$, at 4.24 eV above the ground state minimum. This crossing region was obtained as a converged point on the computed MEP, not as the lowest energy point of the crossing seam. As it is the first funnel reached by the excited molecule, it is of great photophysical relevance.[51,52] Therefore, in this region, a very efficient energy transfer from the S_2 $^1(\pi\pi^*)$ to the S_1 $^1(n\pi^*)$ state occurs, causing an ultrafast depletion of the S_2 $^1(\pi\pi^*)$ excited state.

Once on the S_1 surface, its evolution was characterized by means of the MEP approach, resulting in a barrierless path toward its minimum energy structure ($(S_1)_{min}$), located 3.99 eV adiabatically above the ground state, from which a weak emission may take place. Our computed fluorescence energy (3.37 eV) is in agreement with the experimental values (3.55[29] and 3.59 eV[49]), the discrepancy being attributed to solvent effects, which can cause large blue-shifts in the $^1(n\pi^*)$ states.[53] At the $(S_1)_{min}$ geometry, the T_1 $^3(\pi\pi^*)$ and T_2 $^3(n\pi^*)$ triplet excited states were computed by us at 3.72 and 3.92 eV, respectively, above the ground state minimum. Due to the small energy difference involving the S_1, T_1, and T_2 states in this region ($(S_1)_{min}$), two singlet−triplet crossings $((^1n\pi^*/^3\pi\pi^*)_{STC}$

dx.doi.org/10.1021/jp3091599 | J. Phys. Chem. B 2012, 116, 14000−14007

and ($^1n\pi^*/^3n\pi^*)_{STC}$) may occur, which opens the possibility of population transfer from the S_1 $^1(n\pi^*)$ state to the triplet (T_1 $^3(\pi\pi^*)$ and T_2 $^3(n\pi^*)$) states manifold. Because the strongest spin−orbit coupling occurs between states of different natures,[54,55] it is more likely that the system evolves preferentially to the T_1 hypersurface. Indeed, the spin−orbit coupling (SOC) between S_1 and T_1 was computed to be about 13.4 cm^{-1}, large enough to support fast intersystem crossing from S_1 to the T_1 state (Figure 5); on the other hand, the (S_1/T_1)$_{SOC}$ was computed to be zero, as expected. Once on the lowest triplet state surface, the computed MEP from the (S_1/T_1)$_{SOC}$ structure indicates that the T_1 $^3(\pi\pi^*)$ state evolves in a steepest decent path to its equilibrium geometry ((T_1)$_{min}$), located adiabatically 2.89 eV above the ground state, will be reached, from which it is possible to observe a phosphorescence emission at 2.54 eV.

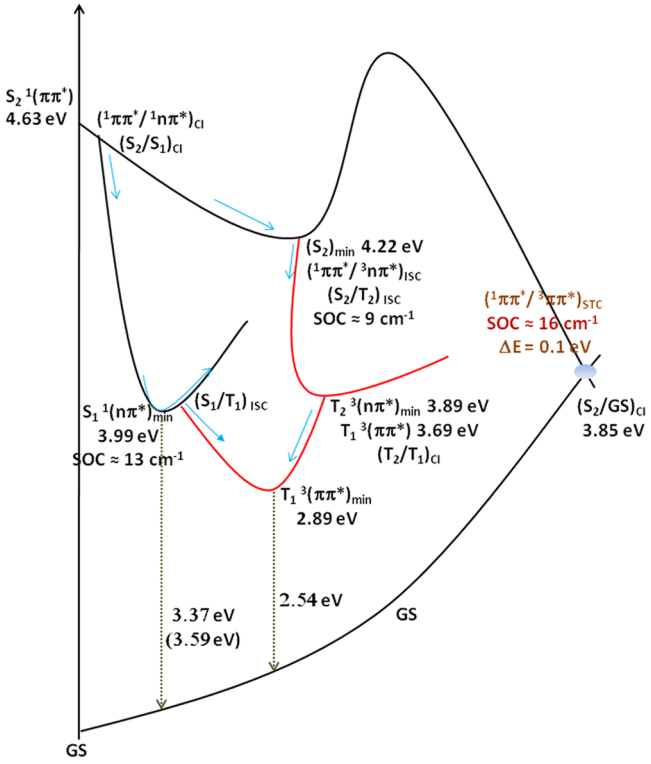

Figure 5. Photochemical scheme to explain the generation of T_1 $^3(\pi\pi^*)$ after irradiation.

The other feature observed in the MEP along the hypersurface of the S_2 $^1(\pi\pi^*)$ state from the FC region (Figure 4) is that it follows in a barrierless path to the S_2 $^1(\pi\pi^*)$ state minimum, $(S_2)_{min}$, placed adiabatically at 4.22 eV above the ground state. From this structure, other possible deactivation mechanisms have been investigated (Figures 4 and 5). For the entire energy profile described by the MEP, the energy difference between the S_1 and S_2 states is very small; besides, the S_1 $^1(n\pi^*)$ and S_2 $^1(\pi\pi^*)$ states are computed be very close energetically at the S_2 $^1(\pi\pi^*)_{min}$ geometry. Since the systems spend more time in the energy region around the minimum of the potential energy surface, it is likely that a population transfer from $(S_2)_{min}$ to S_1 $^1(n\pi^*)$ occurs, leading to $(S_1)_{min}$ via a mechanism similar to that discussed previously for the Franck−Condon region, via a ($^1(n\pi^*)/^1(\pi\pi^*)$)$_{CI}$. The other possible deactivation mechanism could be based on the behavior of adenine,[36] for which a $^1(\pi\pi^*/gs)_{CI}$ is readily accessible. Although the analogous $^1(\pi\pi^*/gs)_{CI}$ (see the SI) has been found for 8-AA in an energy region (3.75 eV adiabatically above the ground state) reasonably close to that computed for the $(S_2)_{min}$ structure, linear interpolation in internal coordinates (LIIC) connecting these two points ($(S_2)_{min}$ and $^1(\pi\pi^*/gs)_{CI}$) suggests that a high energy barrier must be surmounted, disfavoring this relaxation path.

The last possibility is related to the presence of a singlet−triplet crossing, $(^1\pi\pi^*/^3n\pi^*)_{STC}$. At the S_2 $^1(\pi\pi^*)_{min}$ geometry, the T_2 $^3(n\pi^*)$ state is computed to be 0.12 eV (that is, 4.22 eV adiabatically from the ground state) above the S_2 $^1(\pi\pi^*)$ state. Besides the small energy gap, at the S_2 $^1(\pi\pi^*)_{min}$ geometry, the spin−orbit coupling between the S_2 $^1(\pi\pi^*)_{min}$ and T_2 $^3(n\pi^*)$ ($(^1\pi\pi^*/^3n\pi^*)_{STC}$) is computed to be 10 cm^{-1}, large enough for allowing the population transfer from the S_2 $^1(\pi\pi^*)$ state to the T_2 $^3(n\pi^*)$, via the $(^1\pi\pi^*/^3n\pi^*)_{STC}$ intersystem crossing. After 8-AA* enters the triplet manifold, the MEP on the T_2 $^3(n\pi^*)$ state hypersurface leads in a steepest descent path to the $(T_2)_{min}$ structure, placed 3.89 eV adiabatically above the ground state. At this geometry, the T_2 $^3(n\pi^*)$ and T_2 $^3(\pi\pi^*)$ states are degenerate, which makes us proposed the existence of a conical intersection between the T_1 and T_2 states $(^3n\pi^*/^3\pi\pi^*)_{CI}$, resulting in an efficient radiationless deactivation of the T_2 state, by transferring its electronic population to the T_1 state (Table 1 and Figure 2).

No matter how the system evolves, through the singlet or triplet excited states, it will always find a path to reach the lowest T_1 state, which can be used to photosensitize molecular oxygen following a well established mechanism.[56] In the first step, the sensitizer (8-AA) is excited to the S_2 state; then, the S_2 state relaxes to the lowest singlet excited state and to the second triplet excited state (T_2). Either from the S_2 or from the T_2 states, the T_1 state of 8-AA is populated. From the T_1 state, the sensitizer transfers energy to oxygen in its ground state ($^3\Sigma_g^-$), resulting in the desired O_2 $^1\Delta_g$ state. Therefore, 8-AA is a good candidate for photodynamic therapy.

At this point, some comparison with the related species 6-AU[30,50] and adenine is worthwhile.[6] The photophysics of 6-AU, a Type A molecule like 8-AA, is very similar to that described for 8-AA in this work. For 6-AU, the allowed state (S_2), with excitation energy of 4.79 eV, is populated by UV irradiation. The MEP computed on its hypersurface indicates that the system evolves barrierlessly toward the minimum, $(S_2)_{min}$. Once the minimum ($(S_2)_{min}$, 4.35 eV) is reached, two possible mechanisms were considered: singlet and triplet manifolds. In the singlet manifold, similar to 8-AA, $(^1\pi\pi^*/^1n\pi^*)_{CI}$ leads the system to the minimum of the $^1(n\pi^*)$ state, where a crossing with the $^3(\pi\pi^*)$ state, $(^1n\pi^*/^3\pi\pi^*)_{STC}$, opens up the possibility of populating the lowest triplet state. On the other hand, after 6-AU reaches the $(S_2)_{min}$, a $(^1\pi\pi^*/^3n\pi^*)_{STC}$ can be accessed and drives the system to the $(^3n\pi^*/^3\pi\pi^*)_{CI}$, very similar to the mechanism proposed previously by us to the 8-AA.

Adenine, in contrast, has a completely different photophysical behavior when compared to its aza analogue. As mentioned in the Introduction, all DNA nucleobases have an extremely high photostability, implying a low triplet quantum yield. Serrano-Andrés and co-workers studied the mechanisms of populating the triplet excited states[6] and found a similar situation for the triplet manifold. Adenine could populate the triplet excited states in three ways, two being mediated by a $^1(n\pi^*)$ state and one going directly via a $(^1\pi\pi^*/^3\pi\pi^*)_{STC}$ intersystem crossing, near the $(^1\pi\pi^*/gs)_{CI}$. This last relaxation

dx.doi.org/10.1021/jp3091599 | J. Phys. Chem. B 2012, 116, 14000−14007

mechanism is not relevant in 8-AA because of the energetic barrier related to the plane distortion that prevents the S_2 state from reaching the crossing region.

4. CONCLUSIONS

In this work, we studied the mechanisms of population of the lowest triplet state $^3(\pi\pi^*)$ of 8-azaadenine in order to explain the photoproduction of singlet oxygen ($^1\Delta_g$). For this purpose, we used the CASPT2//CASSCF/ANO-L-VDZP protocol to describe stationary equilibrium structures of the ground and excited states and the minimum energy paths, with linear interpolations.

Our results show that, once S_2 $^1(\pi\pi^*)$ is populated by laser irradiation, the system can evolve in a barrierless manner to its planar minimum, S_2 $^1(\pi\pi^*)_{mim}$, as suggested by the computed MEPs, or to a conical intersection region, $(^1\pi\pi^*/^1n\pi^*)_{CI}$. Although two different mechanisms were studied, both are able to populate the lowest triplet state, T_1 $^3(\pi\pi^*)$, which is the state ultimately responsible for the potential applications of 8-AA in photodynamic therapy.

As shown in Figure 4, $(^1\pi\pi^*/^1n\pi^*)_{CI}$ is reached along the MEP, where a transfer of population to the lowest excited state, S_1 ($^1n\pi^*$), leads the system to the state minimum, S_1 $^1(n\pi^*)_{min}$. At this point, a crossing with the lowest triplet state, $(^1n\pi^*/^3\pi\pi^*)_{STC}$, can convert the system to T_1 $^3(\pi\pi^*)$. Alternatively, if the system reaches S_2 $^1(\pi\pi^*)_{mim}$, a crossing with T_2 $^3(n\pi^*)$, $(^1\pi\pi^*/^3n\pi^*)_{STC}$, can efficiently transfer the population to the triplet manifold. Once T_2 is reached, the system evolves to its minimum, T_2 $^3(n\pi^*)_{min}$, where a conical intersection with the lowest triplet, T_1, $(^3n\pi^*/^3\pi\pi^*)_{CI}$, is accessible, also leading to T_1.

■ ASSOCIATED CONTENT

Ⓢ Supporting Information

Cartesian coordinates of the optimized structures. This material is available free of charge via the Internet at http://pubs.acs.org.

■ AUTHOR INFORMATION

Corresponding Author

*E-mail: jpgobbo@iq.usp.br.

Notes

The authors declare no competing financial interest.

■ ACKNOWLEDGMENTS

J.P.G. acknowledges FAPESP (Fundação de Amparo à Pesquisa do Estado de São Paulo) for financial support. A.C.B. acknowledges continuous academic support from CNPq (Conselho Nacional de Desenvolvimento Científico e Tecnológico) and the LCCA (Laboratory of Advanced Scientific Computation) of the University of São Paulo.

■ REFERENCES

(1) Crespo-Hernández, C. E.; Cohen, B.; Hare, P. M.; Kohler, B. *Chem. Rev.* **2004**, *104*, 1977−2019.
(2) Daniels, M.; Hauswirth, W. W. *Science* **1971**, *171*, 675−677.
(3) *Bioinorganic photochemistry*; Morrison, H., Ed.; Wiley: New York, 1990.
(4) Callis, P. R. *Annu. Rev. Phys. Chem.* **1983**, *34*, 329−357.
(5) Serrano-Andrés, L.; Merchán, M.; Borin, A. C. *Proc. Natl. Acad. Sci.* **2006**, *103*, 8691−8696.
(6) González-Luque, R .; Climent, T.; González-Ramirez, I.; Merchán, M.; Serrano-Andrés, L. *J. Chem. Theory Comput.* **2010**, *6*, 2103−2114.
(7) Serrano-Andrés, L.; Merchán, M.; Borin, A. C. *J. Am. Chem. Soc.* **2008**, *130*, 2473−2484.
(8) Serrano-Andrés, L.; Merchán, M.; Borin, A. C. *Chem . Eur. J.* **2006**, *12*, 6559−6571.
(9) Perun, S.; Sobolewski, A. L.; Domcke, W. *J. Phys. Chem. A* **2006**, *110*, 13238−13244.
(10) Marian, C. M. *J. Chem. Phys.* **2005**, *122*, 104314.
(11) Blancafort, L. *J. Am. Chem. Soc.* **2006**, *128*, 210−219.
(12) *Computational Photochemistry*; Olivucci, M., Ed.; Elsevier: Amsterdan, The Netherlands, 1995.
(13) *Conical Intersections*; Domcke, W., Yarkony, D. R, Köppel, H., Eds.; World Scientific: Singapore, 2004.
(14) Favre, A.; Thomas, G. *Annu. Rev. Biophys. Bioeng.* **1981**, *10*, 175−195.
(15) Rist, M. J.; Marino, J. P. *Curr. Org. Chem.* **2002**, *6*, 775−793.
(16) Harada, Y.; Suzuki, T.; Ichimura, T. *J. Phys. Chem. B* **2007**, *111*, 5518−5524.
(17) Kobayashi, T.; Harada, Y.; Suzuki, T.; Ichimura, T. *J. Phys. Chem. A* **2008**, *112*, 13308−13315.
(18) Callis, P. R. *Chem. Phys. Lett.* **1979**, *61*, 563−567.
(19) Cohen, B.; Hare, P. M.; Kohler, B. *J. Am. Chem. Soc.* **2003**, *125*, 13594−13601.
(20) *Organic Molecular Photopysics*; Birks, J. B., Ed.; Wiley: New York, 1977.
(21) Jonas, I.; Michl, J. *J. Am. Chem. Soc.* **1978**, *100*, 6834−6838.
(22) Morgan, J. P.; Daniels, M. *Chem. Phys. Lett.* **1979**, *67*, 533−537.
(23) Holmen, A.; Nordén, B.; Albinsson, B. *J. Am. Chem. Soc.* **1997**, *119*, 3114−3121.
(24) Santhosh, C.; Mishra, P. C. *Spectrochim. Acta* **1991**, *47*, 1685−1693.
(25) Broughton, B. J.; Chaplen, P.; Knowles, P.; Lunt, E.; Pain, D. L.; Wooldridge, K. R. H.; Ford, R.; Marshall, S.; Walker, J. L.; Marshall, D. R. *Nature* **1974**, *251*, 650−652.
(26) El-Brollosy, N. R. *Monatsh. Chem.* **2008**, *139*, 1483−1490.
(27) Montgomery, J. A. *Cancer Res.* **1959**, *19*, 447−463.
(28) Spremulli, E. N.; Crabtree, G. W.; Dexter, D. L.; Chu, S. H.; Farineau, D. M.; Ghoda, L. Y.; McGowan, D. L.; Diamond, I.; Parks, R. E., Jr.; Calabresi, P. *Biochem. Pharmacol.* **1982**, *31*, 2415−2421.
(29) Kobayashi, T.; Kuramochi, H.; Harada, Y.; Suzuki, T.; Ichimura, T. *J. Phys. Chem. A* **2009**, *113*, 12088−12093.
(30) Gobbo, J. P.; Borin, A. C.; Serrano-Andrés, L. *J. Phys. Chem. B* **2011**, *115*, 6423−6251.
(31) Klessinger, M.; Michl, J. *Excited States and Photochemistry of Organic Molecules*; VCH Publishers, Inc.: New York, 1995.
(32) Roos, B. O. In *Advances in Chemical Physics; Ab Initio Methods in Quantum Chemistry II*; Lawley, K. P., Ed.; John Wiley & Sons Ltd.: Chichester, U.K., 1987; Vol. *399*.
(33) Andersson, K.; Malmqvist, P. A.; Roos, B. O. *J. Phys. Chem.* **1992**, *96*, 1218−1226.
(34) Roos, B. O.; Fülscher, M. P.; Malmqvist, P. A.; Merchán, M.; Serrano-Andrés, L. In *Quantum Mechanical Electronic Structure with Chemical Accuracy, Understanding Chemical Reactions*; Langhoff, S. R., Ed.; Kluwer Academic Publishers: Dordretch, The Netherlands, 1995; Vol. *13*.
(35) Roca-Sanjuán, D.; Olaso-González, G.; González-Ramirez, I.; Serrano-Andrés, L.; Merchán, M. *J. Am. Chem. Soc.* **2008**, *130*, 10768−10779.
(36) Serrano-Andrés, L.; Merchán, M. *J. Photochem. Photobiol. C* **2009**, *10*, 21−32.
(37) González-Ramirez, I.; Roca-Sanjuán, D.; Climent, T.; Serrano-Pérez, J. J.; Merchán, M.; Serrano-Andrés, L. *Theor. Chem. Acc.* **2011**, *128*, 705−711.
(38) De Vico, L.; Olivucci, M.; Lindh, R. *J. Chem. Theory Comp.* **2005**, *1*, 1029−1037.
(39) Anglada, J. M.; Bofill, J. M. *J. Comput. Chem.* **1997**, *18*, 992−1003.
(40) Müller, K.; Brown, L. D. *Theor. Chim. Acta* **1979**, *53*, 75−93.
(41) Forsberg, N.; Malmqvist, P. A. *Chem. Phys. Lett.* **1997**, *274*, 196−204.

(42) Ghigo, G.; Roos, B. O.; Malmqvist, P. A. *Chem. Phys. Lett.* **2004**, *396*, 142−149.
(43) Merchán, M.; Serrano-Andrés, L.; Robb, M. A.; Blancafort, L. *J. Am. Chem. Soc.* **2005**, *127*, 1820−1825.
(44) Miertus, S.; Scrocco, E.; Tomasi, J. *Chem. Phys.* **1981**, *55*, 117−129.
(45) Barone, V.; Cossi, M.; Tomasi, J. *J. Comput. Chem.* **1998**, *19*, 404−417.
(46) Karlström, G.; Lindh, R.; Malmqvist, P. A.; Roos, B. O.; Ryde, U.; Veryazov, V.; Widmark, P. O.; Cossi, M.; Schimmelpfennig, B.; Neograd y, P.; Seijo, L. *Comput. Mater. Sci.* **2003**, *28*, 222−239.
(47) Pierloot, K.; Dumez, B.; Widmark, P. O.; Roos, B. O. *Theor. Chim. Acta* **1995**, *90*, 87−114.
(48) Contreras, J. G.; Madariaga, S. T.; Alderete, J. B. *J. Phys. Org. Chem.* **1998**, *11*, 392−396.
(49) Wierzchowski, J.; Wielgus-Kutrowska, B.; Sugar, D. *Biochim. Biophys. Acta* **1996**, *1290*, 9−17.
(50) Etinski, M.; Marian, C. M. *Phys. Chem. Chem. Phys.* **2010**, *12*, 15565−15671.
(51) Michl, J. *In Computational Photochemistry*; Olivucci, M., Ed.; Elsevier: Amsterdam, The Netherlands, 2005; Vol. *16*.
(52) Giussani, A.; Merchán, M.; Roca-Sanjuán, D.; Lindh, R. *J. Chem. Theory Comput.* **2011**, *7*, 4088−4096.
(53) Brealey, G. J.; Kasha, M. *J. Am. Chem. Soc.* **1955**, *77*, 4462−4468.
(54) El-Sayed, M. A. *Acc. Chem. Res.* **1968**, *1*, 8−16.
(55) Marian, C. M. *Comput. Mol. Sci.* **2012**, *2*, 187−203.
(56) DeRosa, M. C; Crutchley, R. J. *Coord. Chem. Rev.* **2002**, *233*, 351−371.